



Unsteady Aerodynamics and Trailing-edge Vortex Sheet of An Airfoil

Xi Xia* and Kamran Mohseni * † ‡

University of Florida, Gainesville, FL, 32603, USA

Unsteady flow models of wings and airfoils have been studied to understand the aerodynamic performance of natural flyers and provide improved maneuverability for micro aerial vehicles (MAVs). Vortex methods have been extensively applied to reduce the dimensionality of these aerodynamic models, based on the proper estimation of the distribution and evolution of the vortices in the wake. In such modeling approaches, one of the most fundamental questions is how the vortex sheets are generated and released from the leading and trailing edges. To study the formation of the trailing-edge vortex sheet, the classical Kutta condition is extended to unsteady situations following the physical sense that flow cannot turn around a sharp edge. This condition can be readily applied to a flat plate or an airfoil with cusped trailing edge since the direction of the forming vortex sheet is known to be tangential to the trailing edge. However, for a non-cusped trailing edge, the direction of the forming vortex sheet is ambiguous. In this study, to remove any ad-hoc condition, a novel analytical formulation is provided to determine the angle of the trailing-edge vortex sheet. The derivation of this equation only requires momentum conservation in the direction normal to the forming vortex sheet. The aerodynamic model together with the proposed unsteady Kutta condition is verified by comparing flow structures and force calculations with experimental results for airfoils in steady and unsteady background flows.

I. Introduction

Mankind has been dreaming to fly for centuries. However, this had not been realized until the pioneers of aerodynamics, such as Kutta and Joukowski,¹ connected lift generation to the flow circulation more than a hundred years ago. All kinds of man-made aerial vehicles have been invented and their flying abilities have been improved dramatically ever since. Over the last several decades, to improve the aerodynamic performance of micro aerial vehicles (MAVs), researchers have focused major attention on studying the aerodynamic secrets of insects and birds that have demonstrated unrivaled maneuverability and agility. To unveil the fundamental aerodynamic mechanisms of the natural flyers, early experimental investigations have attributed this high lift performance to an attached leading edge vortex (LEV). Specifically, the formation and attachment of the leading edge vortex at high angles of attack are related to two-dimensional (2D) stall delaying and three-dimensional (3D) stall prevention, which provide lift enhancement for flapping wings.^{2,3}

In order to accurately capture the flow structures in the wake and compute the lift on a flapping wing, recent modeling attempts have focused extensively on resolving the unsteady dynamics of a flat plate and incorporating vortex dynamics into the wake evolution. Minotti⁴ was the first to develop an unsteady framework for the flow around a pitching flat plate with a single point vortex to model the LEV. However, the single vortex is still modeled in a quasi-steady manner that the vortex is assumed to be stabilized and have constant circulation during pitching motion. Michelin & Smith,⁵ Wang & Eldredge,⁶ and Hemati et al.⁷ modeled the wake using finite sets of point vortices with evolving strengths. Their approach has significantly improved the unsteady capability of the model, while the accuracy is still limited for flow with complex wake patterns due to the rough representation of vortices. Another approach of modeling the wake is to fully represent the vortex sheets in the wake using discretized point vortices or vortex panels as demonstrated

*Department of Mechanical and Aerospace Engineering, University of Florida, Gainesville, FL, 32611-6250, USA.

†Department of Electrical and Computer Engineering, University of Florida, Gainesville, FL, 32611-6250, USA.

‡Institution for Networked Autonomous Systems, University of Florida, Gainesville, FL, 32611-6250, USA. Email address for correspondence: mohseni@ufl.edu

by Katz,⁸ Jones,⁹ Yu et al.,¹⁰ Pullin & Wang,¹¹ Ansari et al.,^{12,13} Shukla & Eldredge,¹⁴ Xia & Mohseni,¹⁵ Ramesh et al.,¹⁶ and Li & Wu.¹⁷ Due to the high resolution of the vortical structures in the wake, the vortex-sheet methods naturally have promising accuracy, whereas the computational cost would grow as time proceeds. Recently, Xia & Mohseni^{18,19} proposed a vortex-amalgamation method which effectively reduces the computational cost for large simulations.

In practice, the unsteady aerodynamic model of a pitching flat plate could apply to a rigid flat wing that has negligible thickness; however, the same technique might not be readily extended to an airfoil since it requires an analytical transformation that maps a circle to the airfoil. While special solutions for certain types of airfoil could exist (such as the Joukowski airfoil), it is generally challenging to find such transformation for an arbitrary shape of airfoil. To address this difficulty, the effect of the airfoil might be substituted by a bound vortex sheet that is located at the surface of the airfoil, the framework of which is similar to vortex panel methods.^{20,8,21,22,9,14,23} Moreover, discretized vortex sheets should be applied to account for the unsteady behaviors of vortex shedding at the leading and trailing edges of the airfoil. This model can be easily adapted from similar models for the flat plate wing¹⁵ with necessary modifications.

The key point of vortex methods is to accurately capture the strength and the geometric configuration of the vortices in the wake. Since the time evolution of free vortical structures can be solved using the Birkhoff-Rott equation,^{24,25,26} the most challenging question to be addressed is how vorticity detaches from the surface of the solid body and enters the fluid. In reality, the generation of vorticity is related to the interaction between fluid and solid boundary that forms the shear layer, which is essentially the product of viscous effect. Since viscosity is ignored in potential flow, a typical solution to that is applying vorticity releasing conditions at the vortex shedding locations of the solid body, e.g. the Kutta condition at a sharp trailing edge. This means that all the viscous effects can be translated into a single condition²⁷ that yields an estimation of the circulation around the body as well as the vorticity created near each vortex shedding location. For trailing edges, the classical 'Kutta condition' has been shown to be effective for steady background flows, thus it is also commonly known as the steady state trailing edge Kutta condition which requires a finite velocity at the trailing edge.^{28,29,30} For a Joukowski airfoil, the steady state Kutta condition is realized by setting the trailing edge to be a stagnation point in the mapped cylinder plane. The effect of this implementation is that the flow from both sides of the trailing edge will be tangential to the edge (or parallel to the center-line of a non-cusped trailing edge), which is consistent with the physical flow near the trailing edge. For the case of a flat plate, this condition will guarantee the streamline emanating from this stagnation point to be inline with the plate, fulfilling the condition proposed in previous studies.^{31,32} In this study, a major task is to extend the steady-state Kutta condition to unsteady situations for cusped and non-cusped trailing edges. Then, flow field and force calculations will be provided and validated against experimental studies.

This paper is organized as follows: Section II introduces the aerodynamic models for a flat plate and an airfoil. Section III provides the unsteady Kutta condition for a flat-plate wing. Section IV proposes an analytical approach to decide the angle of the trailing-edge vortex sheet for non-cusped trailing edge. The flow model and the unsteady Kutta condition are validated through comparisons between simulation and experiment. Finally, concluding remarks are given in Section V.

II. Unsteady Aerodynamic Models

We start by first reviewing our previous study of an analytical potential flow model for a two-dimensional (2D) flat plate wing that undergoes unsteady motions.¹⁵ Potential flow theory is applied primarily because it provides explicit solution of the flow field without solving the full version of the Navier-Stokes equation. The challenge, however, is to deal with the rotational motion of the plate since it is generally difficult to find a potential function for flow with rotation. This is because the vorticity of the entire flow is not zero if the reference frame is body-fixed, meaning that a potential function does not exist. To address this difficulty, a virtual reference frame is applied to serve as an intermediate reference frame, following an earlier work by Minotti.⁴ In this way, it is convenient to obtain the desired complex potential of the original flow through a simple transformation from the potential flow in the virtual frame. However, the same analysis can not be readily extended to the case of an airfoil since this virtual-frame approach only applies to the flat plate. Therefore, to establish a similar potential flow model for an airfoil, we further introduce a vortex-sheet approach which handles the boundary condition of the airfoil by imposing a bound vortex sheet along the surface of the airfoil.

II.A. Review of the 2D potential flow model around a flat plate

Considering the physical flow around a flat plate (shown in Fig. 1), the motion of the plate can be decomposed into a translational motion and a rotational motion around the rotation center. The main task here is to derive a complex potential that properly accounts for these two elementary motions. As discussed previously, the virtual frame proposed by Minotti⁴ is applied here and the resultant complex potential is shown in Eq. 1 by the ‘Translational effect’ and ‘Rotational effect’ terms.

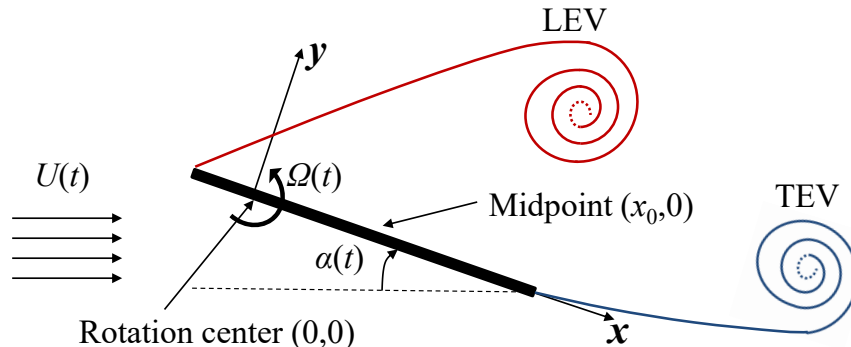


Figure 1. Diagram showing the unsteady flow model of a pitching flat plate.

Next, the effect of the vortical structures in the flow need to be considered. Although both LEV and TEV might exist as shown in Fig. 1, a preliminary model with only one external vortex is presented here without losing generality since more vortices can always be added using the superposition law. This model applies a vortex-sink to represent the major LEV that is centered at z_1 in the physical plane (z -plane) and the vortex and sink intensities of which are Γ_1 and Q , respectively. After performing the Jowkowski transformation between the physical flow around a flat plate and the virtual flow around the corresponding 2D cylinder, the complex potential of the original flow can be derived, in terms of the coordinate of the virtual ζ -plane, as

$$w_\zeta(\zeta) = \underbrace{|U|e^{-i\alpha}(\zeta + x_0) + |U|e^{i\alpha}(a^2/\zeta + x_0)}_{\text{Translational effect}} + \underbrace{i\Omega \frac{x_0^2 - 2a^2 - 2(a^2/\zeta + x_0)^2}{2}}_{\text{Rotational effect}} - \underbrace{\frac{1}{2\pi} [(i\Gamma_0 - Q) \ln(\zeta) + (Q + i\Gamma_1) \ln(\zeta - \zeta_1) + (Q - i\Gamma_1) \ln(\zeta - a^2/\bar{\zeta}_1)]}_{\text{The vortex-sink singularity}}. \quad (1)$$

To improve the accuracy of this model in terms of representing the vortical structures in the wake, Eq. 1 can be easily extended to account for a flat plate with a dynamically growing LEV and TEV by introducing a discretized-vortices model as¹⁵

$$w_\zeta(\zeta) = |U|e^{-i\alpha}(\zeta + x_0) + |U|e^{i\alpha}(a^2/\zeta + x_0) + i\Omega \frac{x_0^2 - 2a^2 - 2(a^2/\zeta + x_0)^2}{2} - \frac{i}{2\pi} \sum_n^N \left[\Gamma_{1n} \ln \left(\frac{\zeta - \zeta_{1n}}{\zeta - a^2/\bar{\zeta}_{1n}} \right) + \Gamma_{2n} \ln \left(\frac{\zeta - \zeta_{2n}}{\zeta - a^2/\bar{\zeta}_{2n}} \right) \right], \quad (2)$$

where N discretized vortices are generated separately at the leading edge and the trailing edge to serve as the shear layers that eventually evolve into larger vortical structures. The evolution of each point vortex should follow the Kirchhoff's law or Biot-Savart law, the detailed formulation of which is given in Xia & Mohseni.¹⁵ Note here that the sink terms in Eq. 1 are dropped out in Eq. 2 for simplicity. It should also be noted that Γ_0 vanishes in this expression because it is assumed that all vortical structures are represented by the $2N$ vortices, thus the bound circulation, $\Gamma_0 - \sum(\Gamma_{1n} + \Gamma_{2n})$, actually equals $-\sum(\Gamma_{1n} + \Gamma_{2n})$ according to Kelvin's circulation theorem. This clearly indicates that $\Gamma_0 = 0$. The corresponding force calculation for this model was not presented here for brevity while more details can be found in Xia & Mohseni.¹⁵

II.B. The unsteady aerodynamic model for an airfoil

The problem of finding a potential flow solution for flow around an airfoil is not fundamentally different from that for a flat plate. This is because both problems share the same governing equation, the Euler equation, and the same boundary condition at the wing or airfoil surface that the normal velocities of the solid and the fluid sides are equal. Therefore, the complex potential in the physical plane for flow over an airfoil might be written, in analogy to Eq. 2, as

$$w(z) = |U|e^{-i\alpha}z - \frac{i}{2\pi} \sum_n^N [\Gamma_{1n} \ln(z - z_{1n}) + \Gamma_{2n} \ln(z - z_{2n})] + w_b(z), \quad (3)$$

where $w_b(z)$ represents the complex potential induced by the airfoil itself. While this term can be found theoretically through the Jowkowski transformation for a flat plate, an analytical solution can not be found for an arbitrary-shape airfoil. Therefore, we place a vortex sheet, which is on the surface of the airfoil, to account for the effect of the airfoil as shown in Fig. 2. In this way, $w_b(z)$ can be expressed as

$$w_b(z) = -\frac{i}{2\pi} \int_s \gamma(s) \ln(z - z'(s)) ds, \quad (4)$$

where $z'(s)$ is the coordinate of any point along the surface of the airfoil, s . Now the task is converted to solving the vortex sheet strength $\gamma(s)$ by satisfying the non-penetration boundary condition,

$$\mathbf{u}(s) \cdot \mathbf{n}(s) = 0, \quad (5)$$

Where $\mathbf{u}(s)$ is the flow velocity at the surface and $\mathbf{n}(s)$ is the normal vector. In complex domain, this can be further written as

$$\text{Re} \left\{ \frac{dw}{dz} \cdot \frac{-idz}{|dz|} \right\} = 0. \quad (6)$$

Here, it should be noted that a general analytical solution to Eq. 6 can not be found. But it can be solved numerically by discretizing the bound vortex sheet into joint vortex panels. Then the problem is converted to solving a linear system represented by the discretized form of Eq. 6. Moreover, we can further extend Eq. 5 to be

$$\mathbf{u}(s) \cdot \mathbf{n}(s) = \mathbf{v}_b(s) \cdot \mathbf{n}(s), \quad (7)$$

where $\mathbf{v}_b(s)$ is the velocity of the solid body element at the surface of the airfoil. By solving Eq. 7 if \mathbf{v}_b is given, the model is capable of handling airfoils with solid-body rotation or even deformation.

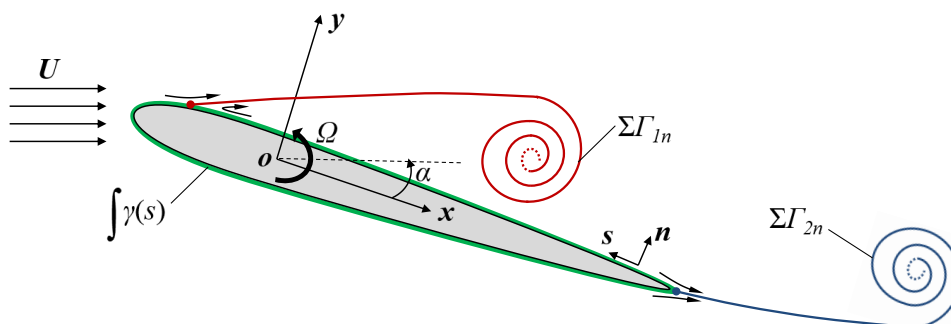


Figure 2. Diagram showing the unsteady flow model of a pitching flat plate.

According to previous studies,^{33,34} the force exerted on the airfoil becomes

$$\mathbf{F} = -\frac{d}{dt} \left(\int_S \mathbf{x} \times \gamma ds + \sum_n^N \mathbf{x}_n \times \Gamma_n \right), \quad (8)$$

where \mathbf{x} is the position vector for any vorticity or circulation, N is the total number of vortices in the wake. Similarly, the torque can be obtained from

$$\boldsymbol{\tau} = -\frac{d}{2dt} \left(\int_S \mathbf{x} \times (\mathbf{x} \times \boldsymbol{\gamma} ds) + \sum^N \mathbf{x}_n \times (\mathbf{x}_n \times \boldsymbol{\Gamma}_n) \right). \quad (9)$$

Equations 8 and 9 enables the force and torque calculations based only on the generation and evolution of the bound vortex sheet and wake vortices.

III. Trailing-edge vortex sheet formation of a flat plate

III.A. Unsteady Kutta condition for cusped trailing edge

The flow field for a flat plate or an airfoil can be calculated using Eq. 2 or Eq. 3 if the intensities and locations of all vortical structures are given. For the bound vortex surrounding the solid body, its effect can be either explicitly expressed for a flat plate or implicitly solved for an airfoil with the non-penetration condition applied at the surface of solid boundary. However, to determine the vortices in the wake, one needs to understand the generation and evolution of the attached and detached vortex sheets. In the Euler limit, since vorticity does not dissipate, it indicates that the circulation of a vortex element can be treated as invariant once it is generated at the leading or trailing edge. Furthermore, the Birkhoff-Rott equation^{24,25,26} can be applied to give the velocity of any vortex element, which is then integrated with respect to time to give the spacial distribution of all existing vortices in the wake. Therefore, the fundamental question here becomes how to decide the rate at which vorticity is being created at the leading or trailing edge. In the current study, the main focus is to understand the vortex-sheet formation at the trailing edge.

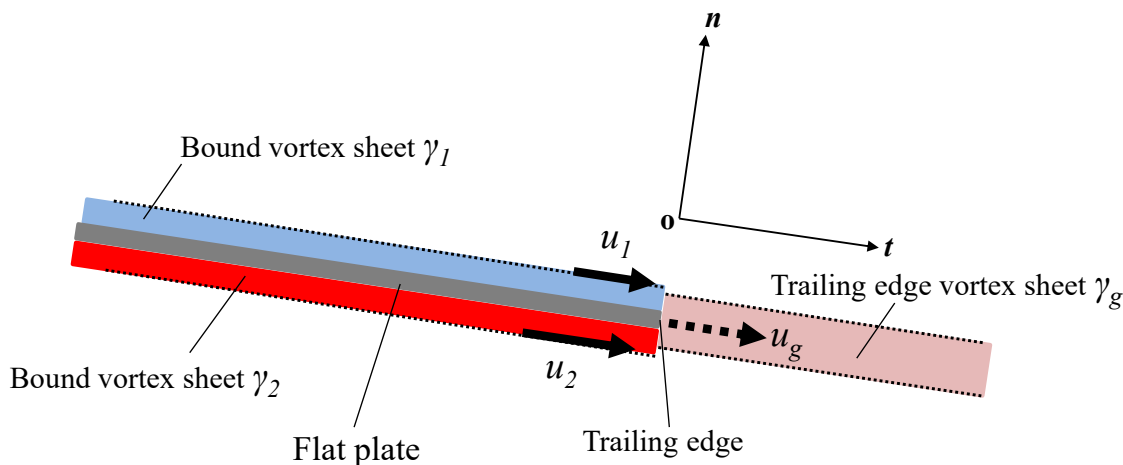


Figure 3. The formation of trailing edge vortex sheet of a flat plate.

Without considering the viscous effect, a typical way of deciding the vortex sheet formation at the trailing edge is the classical steady Kutta condition. The application of this condition for a flat plate or a Joukowski airfoil (with cusped trailing edge) has already been discussed in our previous work.¹⁵ Basically, this condition is equivalent to enforcing a stagnation point at the trailing edge in the transformed cylinder plane (ζ -plane). However, Xia & Mohseni³⁵ later pointed out that a stagnation point generally does not exist at the trailing edge of an unsteady flat plate that has rotary motion. To address this difficulty, they further proposed a modified Kutta condition which relaxes the trailing edge point from totally stagnant to only stagnant in the tangential direction of the surface in the cylinder plane. They have shown that this modified Kutta condition is consistent with the physical meaning of the classical Kutta condition that flow around the sharp edge should be prevented in a reference frame that is fixed to the flat plate. Therefore, this condition can be generalized in the physical plane (the plane of the flat plate or airfoil) as

$$\mathbf{u}_g \cdot \mathbf{n} = 0, \quad (10)$$

where \mathbf{u}_g denotes the de-singularized flow velocity at the trailing edge which is also the velocity of the trailing-edge vortex sheet according to the Birkhoff-Rott equation, and \mathbf{n} represents the vector perpendicular to the trailing-edge tangential vector ($\mathbf{n} \cdot \mathbf{t} = 0$) as shown in Fig. 3. Again, it should be emphasized that Eq. 10 should be implemented in a body-fixed reference frame, which moves and rotates with the flat plate. Since \mathbf{u}_g is affected by all vortical structures and solid body in the flow field, solving Eq. 10 generally requires knowing the entire flow field.

III.B. Simulations and validations

Now, the simulation of a starting flat plate is introduced, as shown in Fig. 4 where a flat plate with 45° angle of attack moves from left to right. The flat plate first accelerates at a rate of 0.625 m/s^2 from rest and then reaches a constant speed of 0.1 m/s . This simulated flow-field snapshots are compared with the experimental images provided by Dickinson & Gotz.³ Again, the potential flow around the flat plate is obtained using complex analysis in virtue of a cylinder plane, which is mapped from the original physical plane using Joukowski transformation. In this way, the flow around the flat plate can be accounted by flow around a cylinder, while discretized point vortices are released at the leading and trailing edges to emulate the free vortex sheets attached to the plate. Here, the unsteady Kutta condition, represented by Eq. 10, should be satisfied at both the leading and trailing edges to determine the strength of the discretized vortex sheets. Although the vortex-sheet formation at the leading edge is not the focus of the current study, it has been demonstrated that a Kutta-like condition would yield good performance for a flat plate with large angle of attack. The good agreement between simulation and experiment qualitatively verifies the flow model and the proposed unsteady Kutta condition. More qualitative validation of the flow model and quantitative validation of the lift calculation for flat plates with different angles of attack and unsteady motions were provided in Xia & Mohseni.¹⁵

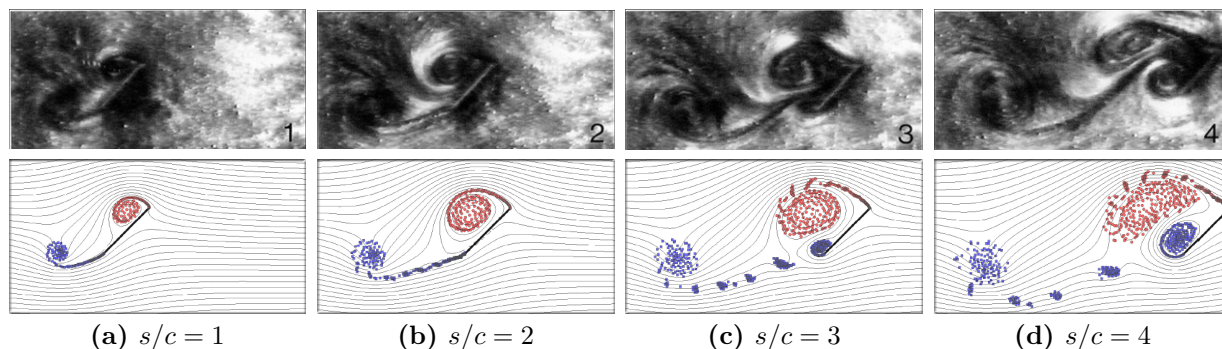


Figure 4. The simulation (bottom) of a starting flat plate at 45° angle of attack is compared with experiment (top) provided by Dickinson & Gotz.³ This plot is adapted from Xia and Mohseni.¹⁵

IV. Trailing-edge vortex sheet formation of an airfoil

IV.A. Unsteady Kutta condition for non-cusped trailing edge

The unsteady Kutta condition (Eq. 10) have been shown to yield promising results in estimating vortex-sheet formation at cusped trailing edges, yet, it was only validated for the situation where a flat plate or a Joukowski airfoil can be mapped to a circle. For a general airfoil which is represented by a bound vortex sheet, Eq. 10 has to be solved in the physical plane to give $\dot{\Gamma}_g$. Here, attention should be focused on the airfoil with non-cusped trailing edge since it could cause additional challenge to solve Eq. 10. As shown in Fig. 5, the two bound vortex sheets at a non-cusped trailing edge are at a certain angle to each other, which is different from the case of a flat plate or a cusped airfoil where the two bound vortex sheets share the same tangent. This inconsistency of the flow direction at the trailing edge creates an ambiguity in deciding the angle of the streamline emanating from the trailing edge, especially for unsteady cases. Actually, this is less of an issue for a steady trailing-edge flow where the shedding of vorticity vanishes. In this case, Poling & Telionis³⁶ pointed out that the emanating streamline bisects the wedge angle of a non-cusped trailing for, otherwise, an unbalance between the upper and lower shear layers near the trailing edge would cause a non-zero vorticity

generation which would violate the steady flow assumption. Apparently, the same argument does not hold for an unsteady trailing-edge flow, where significant mismatch between the emanating streamline and the wedge bisector line has been confirmed experimentally.^{37,36} A prominent theory for the unsteady situation has been proposed by Giesing³⁸ and Maskell³⁹ that the emanating streamline is an extension of the one of the two tangents to the airfoil at the non-cusped trailing edge. Although extensive discussion supporting the Giesing-Maskell model has been provided by Basu & Hancock,⁴⁰ a notable drawback of this model is that it does not reduce to the classic steady condition in the limit of $\dot{\Gamma}_g \rightarrow 0$. Furthermore, Poling & Telionis³⁶ indicated that the Giesing-Maskell model only approximately holds for large $\dot{\Gamma}_g$ values as they observed a smooth change of the trailing-edge streamline direction when $\dot{\Gamma}_g$ is small.

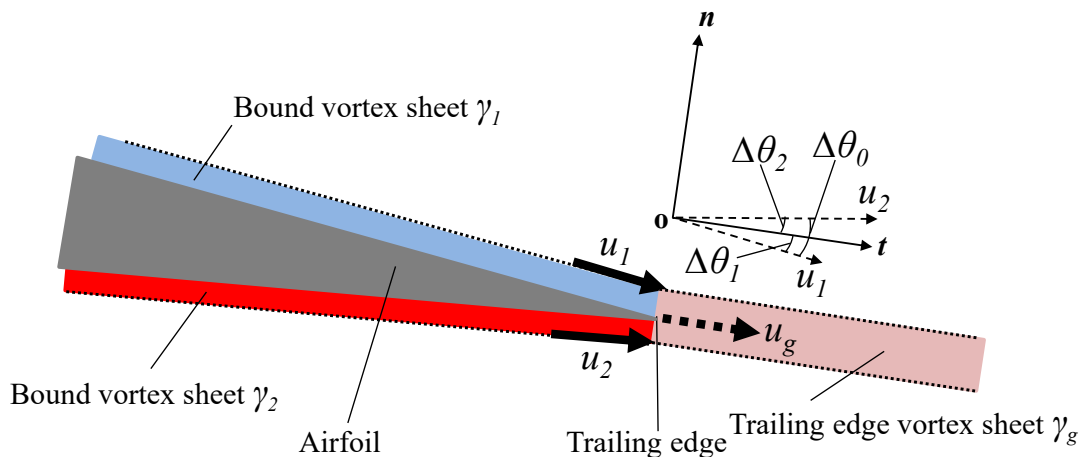


Figure 5. The formation of trailing edge vortex sheet of an airfoil with non-cusped trailing edge.

In this study, to avoid any ad-hoc argument for the unsteady Kutta condition, we propose that the angle of the trailing-edge vortex sheet should be decided in a momentum conservation sense. According to the study of Wu et al.⁴¹ (Eq. 4.121), the momentum conservation of a vortex sheet in the \mathbf{n} direction can be expressed as

$$\llbracket \rho u_n \rrbracket (\bar{u}_n - u_{gn}) = -\llbracket p \rrbracket, \quad (11)$$

where $\llbracket \cdot \rrbracket$ denotes the jump of a quantity across the vortex sheet, $u_n = \mathbf{u} \cdot \mathbf{n}$, $\bar{u}_n = (u_{1n} + u_{2n})/2$, and $u_{gn} = \mathbf{u}_g \cdot \mathbf{n}$. They further showed that $\llbracket p \rrbracket = 0$ always holds for a free vortex sheet which has no surface tension. Since the vortex sheet generated at the trailing edge is a free vortex sheet, $\llbracket p \rrbracket = 0$ should always be satisfied and this is also consistent with the requirement of the classical Kutta condition. According to the properties of the vortex sheets at the trailing edge, $\gamma_1 = -u_1$ and $\gamma_2 = u_2$. As a result, Eq. 11 becomes

$$(\gamma_2 \sin \Delta\theta_2 + \gamma_1 \sin \Delta\theta_1)(\gamma_2 \sin \Delta\theta_2 - \gamma_1 \sin \Delta\theta_1)/2 = 0, \quad (12)$$

where $\gamma_2 \geq 0$ and $\gamma_1 \leq 0$ are valid according to the physical flow at the trailing edge. Therefore, Eq. 12 could be simplified to

$$\gamma_2 \sin \Delta\theta_2 + \gamma_1 \sin \Delta\theta_1 = 0 \quad \text{with} \quad \Delta\theta_1 \cdot \Delta\theta_2 \geq 0, \quad (13)$$

or

$$\gamma_2 \sin \Delta\theta_2 - \gamma_1 \sin \Delta\theta_1 = 0 \quad \text{with} \quad \Delta\theta_1 \cdot \Delta\theta_2 < 0. \quad (14)$$

Without losing generality, we could also assume that $\gamma_2 \geq -\gamma_1$. Further noting that

$$\Delta\theta_1 + \Delta\theta_2 = \Delta\theta_0, \quad (15)$$

where $\Delta\theta_0$ is the finite angle of the trailing edge, we can easily prove that a solution to Eq. 14 does not exist. Therefore, $\Delta\theta_1$ and $\Delta\theta_2$ can be decided by solving the combined equations 13 and 15.

To this end, several important notes should be made about this new angle model for the unsteady Kutta condition. First of all, it can be readily verified that the steady Kutta condition can be achieved when $\gamma_2 = -\gamma_1$. This means that the new model is consistent for both steady and unsteady trailing edge flows. Second, the denial of Eq. 14 as a possible solution indicates that both $\Delta\theta_1$ and $\Delta\theta_2$ are non-negative angles.

This means that the momentum conservation actually dictates that the direction of the forming vortex sheet should not exceed the two tangential directions of the trailing edge surfaces. Therefore, this implication is consistent with the physical sense of the classical Kutta condition that ‘flow cannot turn around a sharp edge’. Moreover, as $\Delta\theta_0$ goes to zero, it yields $\Delta\theta_1 = 0$ and $\Delta\theta_2 = 0$ which is the limiting case of a flat plate or a cusped trailing edge. Finally, with $\Delta\theta_1$ and $\Delta\theta_2$ determined, Eq. 10 can be again applied as the unsteady Kutta condition to evaluate $\dot{\Gamma}_g$ and the performance of the this model will be verified next.

IV.B. Simulations and validations

To verify the flow model together with the proposed unsteady Kutta condition for a non-cusped airfoil, a NACA 0012 airfoil in steady background flow is simulated at various angles of attack. The airfoil, with a chord length of 0.1 m, impulsively starts and then reaches a constant speed corresponding to a Reynolds number of 5×10^4 . Since this study only focuses on the formation of trailing edge vortex-sheet formation, the flow separation near the leading edge is neglected. For this reason, only the small angle-of-attack situation is considered here as the flow is mostly attached in this case until stall occurs. Again, the unsteady Kutta condition is implemented by first solving the angle of the forming vortex sheet using equations 13 and 15, and then enforcing Eq. 10 to obtain $\dot{\Gamma}_g$. The steady-state lift coefficient resulted from this simulation is plotted in Fig. 6 and compared with experimental data. It can be verified that the lift calculation has good agreement with experiment up to about 15° angle of attack where lift stalls due to leading-edge flow separation, which has not been modeled in this study.

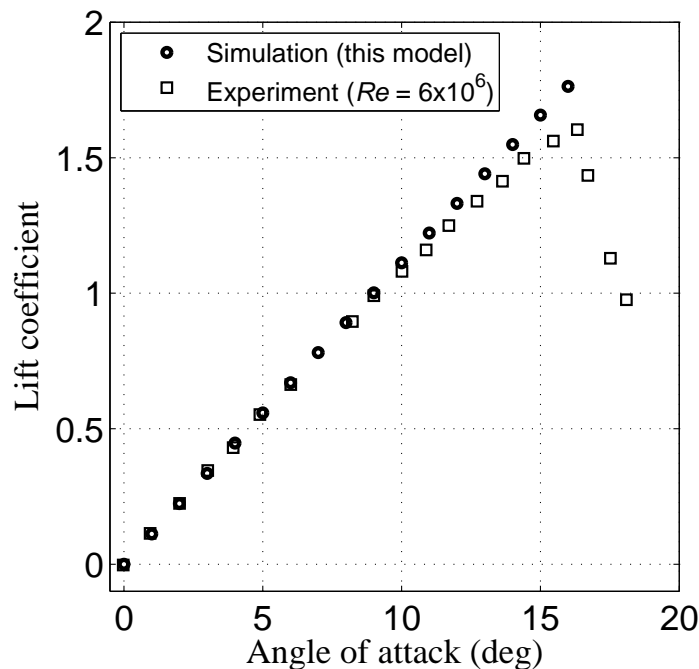


Figure 6. Lift coefficient vs. angle of attack for a NACA 0012 airfoil. The experimental data are corresponding to $Re = 6 \times 10^6$.

Next, the aerodynamic model and unsteady Kutta condition for an airfoil is further verified through the simulation of a NACA 0012 airfoil with unsteady motions. The movement of the airfoil follows a combined pitching and heaving pattern which is adapted from the experiment conducted by Read et al.⁴² For all testing cases, the chord length, c , and the towing speed, U , are fixed at 0.1 m and 0.4 m/s, respectively. This corresponds to a Reynolds number of 4×10^4 . The phase difference angle, ψ , between the pitching and heaving motions is set to 90° in all circumstances. The parameters characterizing the motion of the airfoil are the Strouhal number, St , and the amplitude of angle-of-attack, α_{max} , which could be adjusted by controlling the pitch and heave motions. Fig. 7 shows the comparison of the flow structures between this simulation and the flow visualization image of the original experiment for a sample case with $St = 0.45$ and $\alpha_{max} = 30^\circ$. The good matching of the wake patterns provides qualitative support for the flow model and

the simulation.

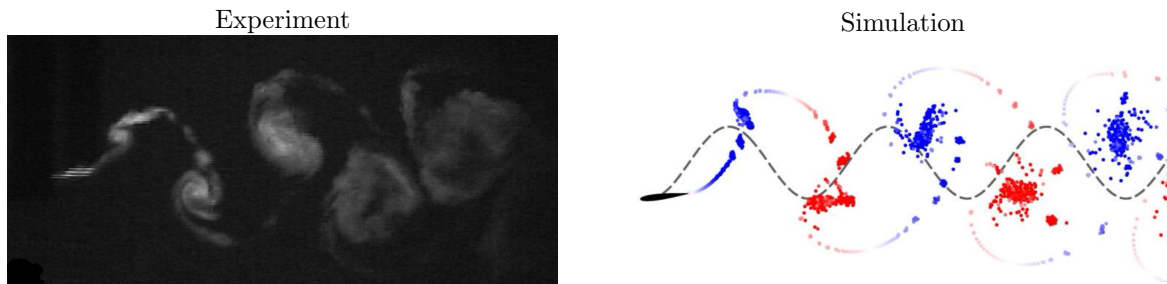


Figure 7. Comparison between flow visualization and simulation. The NACA 0012 airfoil is towed from right to left with $St = 0.45$ and $\alpha_{max} = 30^\circ$. The flow visualization image is adapted from Schouveiler et al.⁴³

Fig. 8 shows the time evolution of the instantaneous force vectors for pitching and heaving motions of the airfoil similar to Fig. 7, but with different St and α_{max} values. The results show reasonable agreement of the force magnitude and direction between experiment and simulation. This quantitatively validates the performance of the aerodynamic model and vorticity generation conditions for an non-cusped airfoil undergoing highly unsteady motions. However, since the leading edge vortex sheet has not been considered in this model, the simulation results tend to yield less accuracy for the cases with larger α_{max} or St where leading edge separation is more likely to take place.

The complexity of the airfoil motion can be further increased by adding oscillatory in-line motion based on the pitching and heaving motions introduced above. Two typical motions of such kind were described by Izraelevitz & Triantafyllou,⁴⁴ namely, the bird-like forward biased downstroke and the turtle-like backward moving downstroke. The trajectories of these motions are shown in Fig. 9, with the simulated flow field showing the vortical structures in the wake after the completion of one downstroke cycle. The airfoil used here is a NACA 0013 type with chord length of 0.055 m. The Reynolds number is fixed at 11000 which is calculated based on a constant towing speed. The amplitude of the heave motion h is set to be equivalent to the chord length c for all situations. Note that in both cases, St and α_{max} are fixed at 0.3 and 25° , respectively. The only parameter to distinguish the two cases is the stroke angle, β , which is related to the ratio between y and x position in the carriage reference frame. The interested readers are referred to Izraelevitz & Triantafyllou⁴⁴ for more details of the original experiment.

Fig. 10 shows the evolution of force and torque coefficients during each cycle of the prescribed motion. Again, the simulation results generally well capture the magnitude and trend of the experimental curves, verifying the correctness of the flow model and the unsteady Kutta condition. It should not be ignored that the simulation tends to over-predict the experimental results of the x -direction force coefficient (C_x). This could be caused by the viscous effect that is not captured in this inviscid flow model. Specifically, it is likely to be the consequence of leading edge separation which has not been modeled. For the same reason, Fig. 10(b) shows better matching of C_x compared with Fig. 10(a), since the airfoil motion in Fig. 9(a) potentially causes more leading-edge separation than that in Fig. 9(b). Furthermore, we can also observe that the bird-like downstroke mainly provides net force in y -direction while the turtle-like downstroke generates about equal net force in both directions. Physically, y -direction and x -direction forces corresponds to lift and thrust respectively. Therefore, we can conclude that the bird-like downstroke is more effective in providing lift enhancement while the turtle-like downstroke is more balanced in lift and thrust generation.

Finally, Fig. 11 shows the variation history of the angle of the trailing-edge vortex sheet, θ_g , for these two motions. Note that the two tangents to the trailing edge surfaces correspond to the angles of $-\Delta\theta_0/2$ and $\Delta\theta_0/2$, respectively. According to Fig. 11, the proposed unsteady Kutta condition dictates that $-\Delta\theta_0/2 \leq \theta_g \leq \Delta\theta_0/2$, which is consistent with the physical interpretation of the Kutta condition that ‘flow cannot turn around the sharp edge’. Moreover, Fig. 11 shows that θ_g changes continuously between the two tangents of the trailing edge. This confirms the experimental observation of Poling and Telionis³⁶ that a smooth change of the trailing-edge streamline direction is possible.

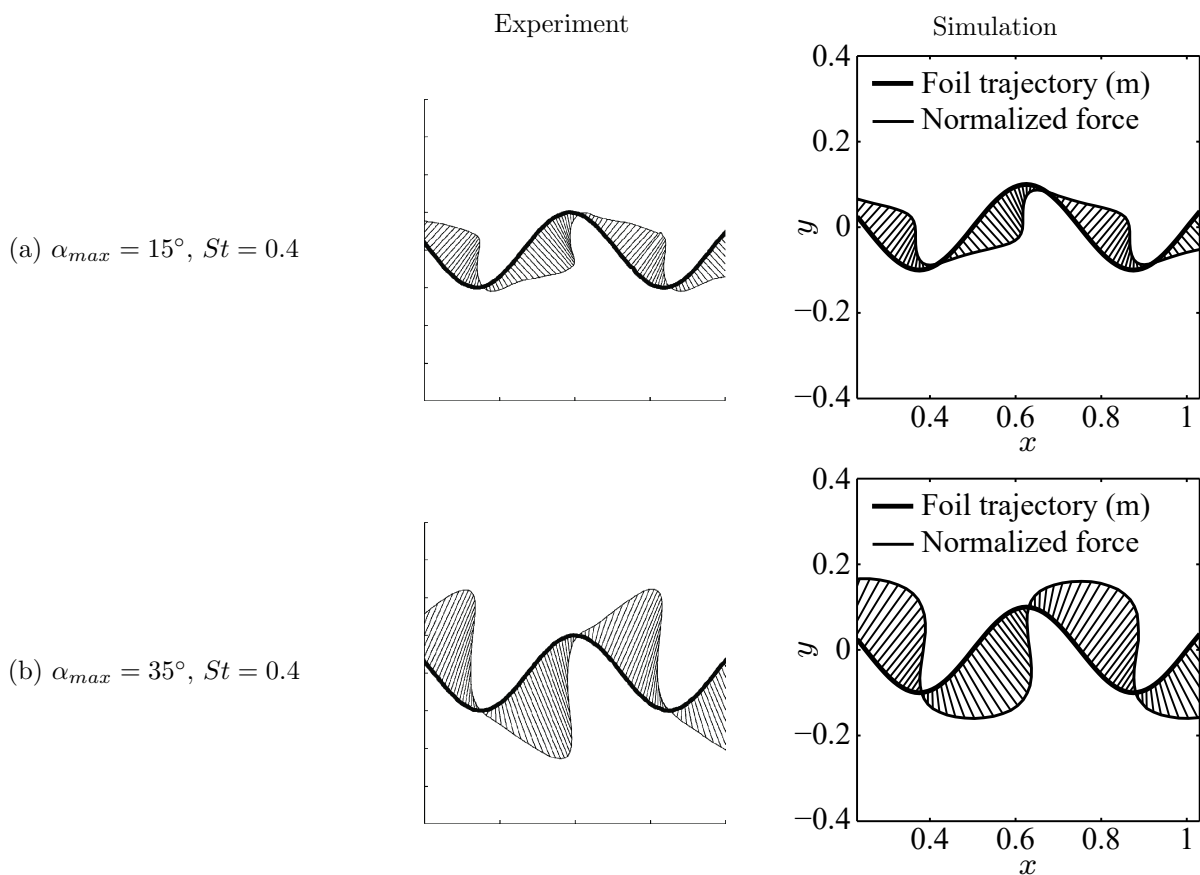


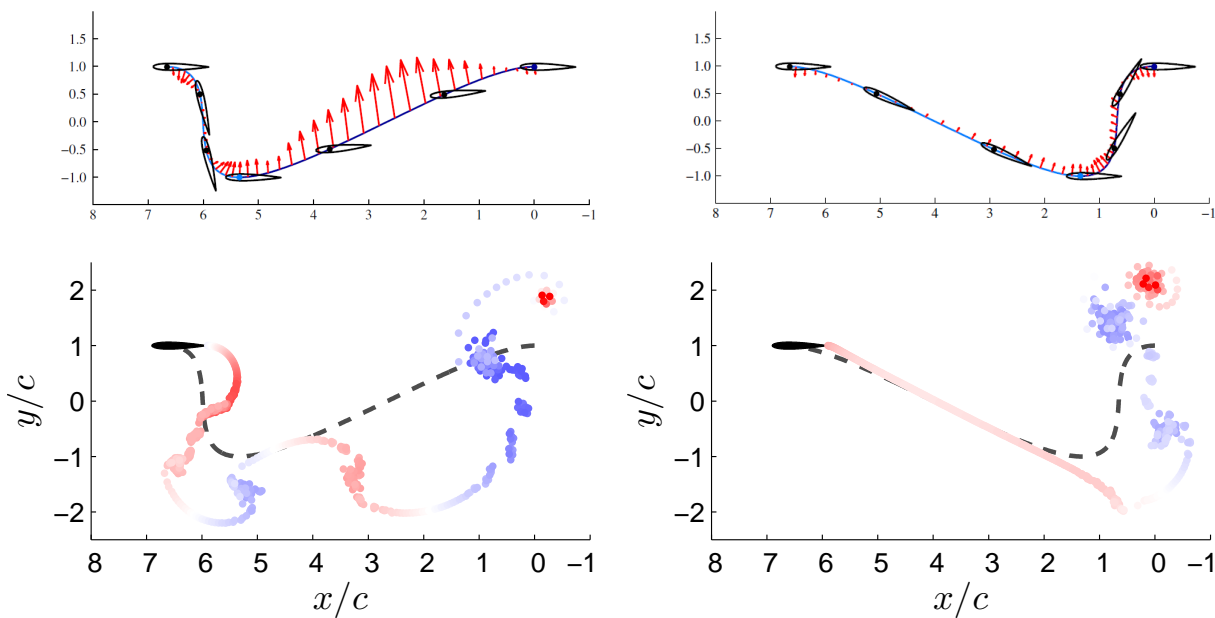
Figure 8. Comparison of instantaneous thrust vectors between experiment and simulation for a NACA 0012 airfoil with various maximum angles of attack α_{max} and Strouhal number St . The experiment results are adapted from the reference.⁴²

V. Conclusion

An unsteady aerodynamic model for an airfoil is derived based on the dynamics of the bound vortex sheet and the wake vortices. The vorticity generation mechanism at the trailing edge is studied since it is essential to predict the vortex shedding and evolution processes in the wake. This can be solved by applying the unsteady Kutta condition, which is extended from the classical Kutta condition based on the physical sense that flow cannot turn around a sharp edge. The validity of this condition has been verified by simulations of a flat plate. However, applying the unsteady Kutta condition to an airfoil with non-cusped trailing edge is not straightforward, as the angle of the forming vortex sheet could change between the two tangential directions of the trailing edge. Realizing that any arbitrary choice for the vortex-sheet angle would be ad-hoc, this study proposes to determine this angle based on the momentum conservation in the direction normal to the forming vortex sheet. As a result, the angle of the emanating vortex sheet can be mathematically decided from the two bound vortex sheets at the trailing edge. Furthermore, the solution of this model only allows the angle of the forming vortex sheet to change between the two tangential directions of the trailing edge, which analytically explained why ‘flow cannot turn around a non-cusped edge’. Airfoils in various steady and unsteady flows are simulated and the flow field and force calculations are compared with experimental data. The good agreement between simulation and experiment confirms the validity of the proposed unsteady Kutta condition and the vortex-sheet based aerodynamic model.

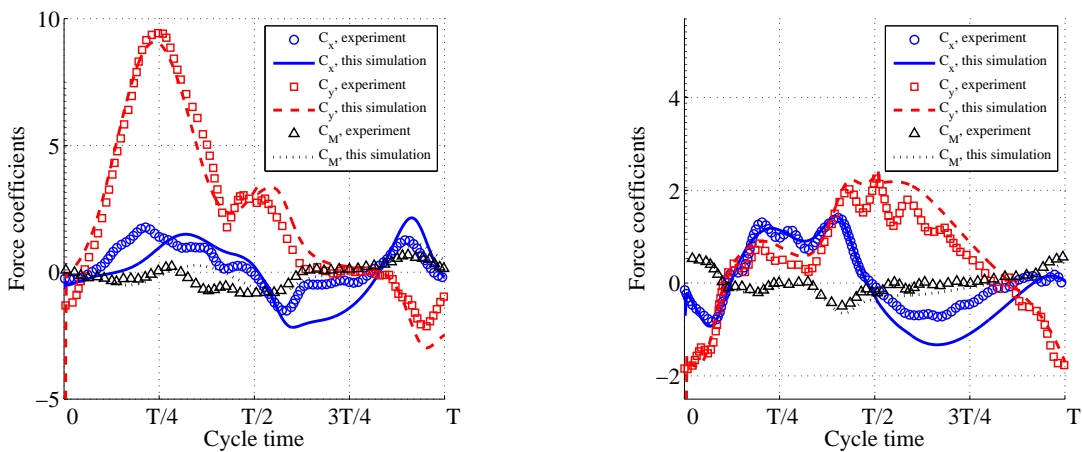
References

- ¹Milne-Thomson, L. M., *Theoretical Hydrodynamics*, Dover, New York, 1958.



(a) Bird-like forward biased downstroke (b) Turtle-like backward moving downstroke

Figure 9. (Top) The trajectories of different flapping motion adapted from the experiment by Izraelevitz & Triantafyllou.⁴⁴ (Bottom) Simulated flow field patterns that correspond to the prescribed trajectories.



(a) Bird-like forward biased downstroke (b) Turtle-like backward moving downstroke

Figure 10. Comparison between the measured force coefficients (C_x , C_y , and C_M) and calculated force coefficients from this simulation for the airfoil movements described in Fig. 9 (Experimental data from Izraelevitz & Triantafyllou⁴⁴).

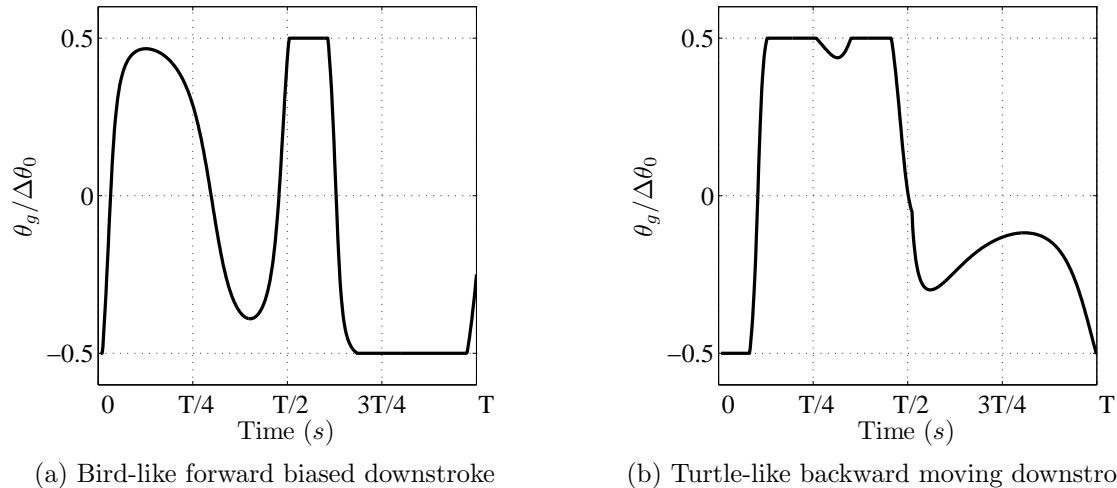


Figure 11. The evolution of the angle of the forming vortex sheet, θ_g , at the trailing edge for the airfoil movements described in Fig. 9. Note that the angles of the two tangential surfaces at the trailing edge are $-\Delta\theta_0/2$ and $\Delta\theta_0/2$, respectively.

- ²Ellington, C., “The aerodynamics of hovering insect flight. IV. Aerodynamic mechanisms,” *Phil. Trans. R. Soc. Lond. B*, Vol. 305, 1984, pp. 79–113.
- ³Dickinson, M. and Gotz, K., “Unsteady aerodynamic performance of model wings at low Reynolds numbers,” *J. Exp. Biol.*, Vol. 174, 1993, pp. 45–64.
- ⁴Minotti, F. O., “Unsteady two-dimensional theory of a flapping wing,” *PHYSICAL REVIEW E*, Vol. 66, 2002, pp. (051907) 1–10.
- ⁵Michelin, S. and Smith, S. L., “An unsteady point vortex method for coupled fluid-solid problems,” *Theor. Comput. Fluid Dyn.*, Vol. 23, 2009, pp. 127–153.
- ⁶Wang, C. and Eldredge, J. D., “Low-order phenomenological modeling of leading-edge vortex formation,” *Theoretical and Computational Fluid Dynamics*, Vol. 27, No. 5, 2013, pp. 577–598.
- ⁷Hemati, M. S., Eldredge, J. D., and Speyer, J. L., “Improving vortex methods via optimal control theory,” *Journal of Fluids and Structures*, Vol. 49, 2014, pp. 91–111.
- ⁸Katz, J., “A discrete vortex method for the non-steady separated flow over an airfoil,” *Journal of Fluid Mechanics*, Vol. 102, 1981, pp. 315–328.
- ⁹Jones, M. A., “The separated flow of an inviscid fluid around a moving flat plate,” *Journal of Fluid Mechanics*, Vol. 496, 2003, pp. 405–441.
- ¹⁰Yu, Y., Tong, B., and Ma, H., “An analytic approach to theoretical modeling of highly unsteady viscous flow excited by wing flapping in small insects,” *Acta Mechanica Sinica*, Vol. 19, 2003.
- ¹¹Pullin, D. and Wang, Z., “Unsteady forces on an accelerating plate and application to hovering insect flight,” *J. Fluid Mech.*, Vol. 509, No. 07, 2004, pp. 1–21.
- ¹²Ansari, S., Zbikowski, R., and Knowles, K., “A nonlinear unsteady aerodynamic model for insect-like flapping wings in the hover: Part I. Methodology and analysis,” *Proceedings IMechE Part G: Journal of Aerospace Engineering*, Vol. 220, No. G2, 2006, pp. 61–83.
- ¹³Ansari, S., Zbikowski, R., and Knowles, K., “Non-linear unsteady aerodynamic model for insect-like flapping wings in the hover. Part 2: Implementation and validation,” *Proceedings IMechE Part G: Journal of Aerospace Engineering*, Vol. 220, No. G3, 2006, pp. 169–186.
- ¹⁴Shukla, R. K. and Eldredge, J. D., “An inviscid model for vortex shedding from a deforming body,” *Theoretical and computational fluid dynamics*, Vol. 21, No. 5, 2007, pp. 343–368.
- ¹⁵Xia, X. and Mohseni, K., “Lift evaluation of a two-dimensional pitching flat plate,” *Physics of Fluids*, Vol. 25, No. 9, 2013, pp. 091901.
- ¹⁶Ramesh, K., Gopalarathnam, A., Granlund, K., Ol, M. V., and Edwards, J. R., “Discrete-vortex method with novel shedding criterion for unsteady aerofoil flows with intermittent leading-edge vortex shedding,” *Journal of Fluid Mechanics*, Vol. 751, 2014, pp. 500–538.
- ¹⁷Li, J. and Wu, Z., “Unsteady lift for the Wagner problem in the presence of additional leading/trailing edge vortices,” *Journal of Fluid Mechanics*, Vol. 769, 2015, pp. 182–217.
- ¹⁸Xia, X. and Mohseni, K., “Modeling of 2D unsteady motion of a flat plate using potential flow,” *Proceedings of the AIAA Applied Aerodynamics Conference*, No. 2013-2819, San Diego, CA, USA, June 24-27 2013.
- ¹⁹Xia, X. and Mohseni, K., “Enhancing lift on a flat plate using vortex pairs generated by synthetic jet,” *Proceedings of the AIAA Aerospace Sciences Meeting*, No. 2015-1932, Kissimmee, FL, USA, January 5-9 2015.

²⁰Morino, L. and Kuo, C., "Subsonic Potential Aerodynamics for Complex Configurations: A General Theory," *AIAA Journal*, Vol. 12, No. 2, 1974, pp. 191-197.

²¹Katz, J. and Plotkin, A., *Low-Speed Aerodynamics: From Wing Theory to Panel Methods*, McGraw-Hill College, 1991.

²²Zhu, Q., Wolfgang, M. J., Yue, D. K. P., and Triantafyllou, M. S., "Three-dimensional flow structures and vorticity control in fish-like swimming," *Journal of Fluid Mechanics*, Vol. 468, 2002, pp. 1-28.

²³Pan, Y., Dong, X., Zhu, Q., and Yue, D. K. P., "Boundary-element method for the prediction of performance of flapping foils with leading-edge separation," *Journal of Fluid Mechanics*, Vol. 698, 2012, pp. 446-467.

²⁴Lin, C. C., "On the motion of vortices in two dimensions-I. Existence of the Kirchhoff-Routh function," *Physics*, Vol. 27, 1941, pp. 570-575.

²⁵Birkhoff, G., "Helmholtz and Taylor instability," *Proc. Symp. in Applied Mathematics*, Vol. 13, 1962, pp. 55-76.

²⁶Rott, N., "Diffraction of a weak shock with vortex generation," *Journal of Fluid Mechanics*, Vol. 1, 1956, pp. 111-128.

²⁷Crighton, D., "The Kutta condition in unsteady flow," *Ann. Rev. Fluid Mech.*, Vol. 17, 1985, pp. 411-445.

²⁸Saffman, P. and Sheffield, J., "Flow over a wing with an attached free vortex," *Studies in Applied Mathematics*, Vol. 57, 1977, pp. 107-117.

²⁹Huang, M.-K. and Chow, C.-Y., "Trapping of a free vortex by Joukowski airfoils," *AIAA*, Vol. 20, No. 3, 1981.

³⁰Mourtos, N. and Brooks, M., "Flow past a flat plate with a vortex/sink combination," *Journal of Applied Mechanics*, Vol. 63, 1996, pp. 543-550.

³¹Chen, S. and Ho, C. M., "Near wake of an unsteady symmetric airfoil," *Journal of Fluids and Structures*, Vol. 1, 1987, pp. 151-164.

³²Poling, D. and Telionis, D., "The trailing edge of a pitching airfoil at high reduced frequency," *Journal of Fluid Engineering*, Vol. 109, 1987, pp. 410-414.

³³Wu, J., "Theory for aerodynamic force and moment in viscous flows," *AIAA Journal*, Vol. 19, 1981, pp. 432-441.

³⁴Eldredge, J. D., "A reconciliation of viscous and inviscid approaches to computing locomotion of deforming bodies," *Experimental Mechanics*, Vol. 50, No. 9, 2010, pp. 1349-1353.

³⁵Xia, X. and Mohseni, K., "A Flat Plate with Unsteady Motion: Effect of Angle of Attack on Vortex Shedding," AIAA paper 2014-0746, National Harbor, MD, Jan 13-17 2014.

³⁶Poling, D. R. and Telionis, D. P., "The response of airfoils to periodic disturbances - The unsteady Kutta condition," *AIAA Journal*, Vol. 24, No. 2, 1986, pp. 193-199.

³⁷Ho, C. M. and Chen, S. H., "Unsteady condition of a plunging airfoil," *Unsteady Turbulent Shear Flows*, 1981, pp. 197-200.

³⁸Giesing, J. P., "Vorticity and Kutta condition for unsteady multienergy flows," *ASME Journal of Applied Mechanics*, Vol. 36, No. 3, 1969, pp. 608-613.

³⁹Maskell, E. C., "On the Kutta-Joukowski condition in two-dimensional unsteady flow," *Unpublished note, Royal Aircraft Establishment, Farnborough, England*, 1971.

⁴⁰Basu, B. C. and Hancock, G. J., "The unsteady motion a two-dimensional aerofoil in incompressible inviscid flow," *Journal of Fluid Mechanics*, Vol. 87, 1978, pp. 159-178.

⁴¹Wu, J. Z., Ma, H. Y., and Zhou, M. D., *Vorticity and Vortex Dynamics*, Springer, 2006.

⁴²Read, D. A., Hover, F. S., and Triantafyllou, M. S., "Forces on oscillating foils for propulsion and maneuvering," *Journal of Fluids and Structures*, Vol. 17, No. 1, 2003, pp. 163-183.

⁴³Schouveiler, L., Hover, F. S., and Triantafyllou, M. S., "Performance of flapping foil propulsion," *Journal of Fluids and Structures*, Vol. 20, No. 7, 2005, pp. 949-959.

⁴⁴Izraelevitz, J. S. and Triantafyllou, M. S., "Adding in-line motion and model-based optimization offers exceptional force control authority in flapping foils," *Journal of Fluid Mechanics*, Vol. 742, 2014, pp. 5-34.